SHALLOW-WATER SPECTRAL SHAPES

JANE MCKEE SMITH

Coastal and Hydraulics Laboratory, US Army Engineer Research and Development Center, 3909 Halls Ferry Road, Vicksburg, MS 39180-6199, USA

Laboratory flume observations and Boussinesq model simulations of wave transformation are used to investigate the evolution of spectral shapes in shallow water. Wave spectra of nonlinear, shallow-water waves both inside and outside the surf zone evolve to the same equilibrium shape (single-peak, double-peak, broad, and narrow incident spectra). The equilibrium shape consists of two slopes, $k^{-4/3}$ for $kd < 1$ and $k^{-5/2}$ for $kd > 1$. Broad incident spectra or multi-peaked spectra evolve to equilibrium over shorter distances than narrow incident spectra. Likewise, the evolution distances shorten as nonlinearity increases. The one-dimensional, time-domain Boussinesq model of Nwogu and Demirbilek (2001) reproduced the spectral evolution both inside and outside the surf zone. The model also simulated the equilibrium range spectral shapes for $kd < 1.5$. Similar to deepwater spectral evolution, the equilibrium range in shallow water is driven by the nonlinear wave-wave interactions. The evolution in spectral shape from strong harmonic peaks to an equilibrium shape reflects the change in wave shape from a vertical asymmetry to a horizontal asymmetry.

1. Introduction

Wave spectra develop a flattened, featureless shape in shallow water, if the waves are sufficiently large and evolution distances sufficiently long (Eldeberky and Battjes 1996; Herbers and Burton 1997). Initially, distinct harmonics develop, but over some propagation distance, the high-frequency portion of the spectrum evolves to an equilibrium shape with no recurrence of the distinct harmonics (Elgar et al. 1990). Both narrow and broad incident spectra evolve to approximately the same equilibrium shape. Smith and Vincent (2002) identified two high-frequency spectral equilibrium ranges in the surf zone: 1) $k^{-4/3}$ for $kd < 1$, where k is wave number and d is water depth, and 2) $k^{-5/2}$ for $kd > 1$. Zakharov (1999) theoretically derived the first range from the kinetic equation, assuming shallow water. Toba (1973) and Resio et al. (2001) identified the second range in deep and intermediate water depths, respectively, based on observations and numerical simulations. Smith and Vincent hypothesized that strong nonlinear wave-wave interactions led to the development of the equilibrium ranges. They examined 1500 laboratory and field spectra measured in the surf zone. Their work was motivated by observations of the preferential decay of high-frequency peaks for multiple wave trains in the surf zone (Smith and Vincent 1992).

In this study, laboratory observations over a sloping bottom in a flume are used to investigate the spectral evolution outside the surf zone. Both single- (broad and narrow energy distributions) and double-peaked wave spectra were simulated. Double-peaked spectra demonstrate the effect of strong nonlinear interactions as reflected in the order one changes in energy density at the higher frequency peak. In addition to the analysis of the laboratory measurements, numerical calculations of the three-wave interactions are made using the Boussinesq model of Nwogu and Demirbilek (2001). Model results are verified with the measurements and then the model is applied to investigate the evolution of the equilibrium range over a number of wavelengths on a flat bottom.

The spectral distribution of wave energy in shallow water impacts the forcing functions for nearshore circulation, wave setup, and sediment transport. Nearshore spectral wave transformation models routinely neglect wave-wave interactions or parameterize them (Booij et al. 1999) to produce harmonics based on wave breaking on a steep slope (e.g., Eldeberky and Battjes 1996). This parametric approach has had limited success. The purpose of this paper is to quantify the equilibrium spectral shape outside the surf zone, determine the distances over which evolution occurs, and assess to what degree existing models of nonlinear, shallow-water wave-wave interactions represent the development of the observed equilibrium range.

2. Laboratory Experiments

The laboratory experiments were conducted at the US Army Engineer Research and Development Center, Coastal and Hydraulics Laboratory. A schematic of the wave flume is shown in Figure 1. The flume is 0.45 m wide, 45.7 m long, and 0.9 m deep. The flume has a 1:30 slope that begins 21 m from the wave generator. The flume is glass walled with a smooth, concrete bottom. All tests were run with a water depth of 61 cm. Waves were measured with 10 capacitance wave gauges. Gauge 1 was located 6.7 m from the wave generator and the other gauges were grouped on the slope (Figure 1). Gauge depths were 61, 30, 24, 21, 18, 15, 12, 9, 7, and 5 cm.

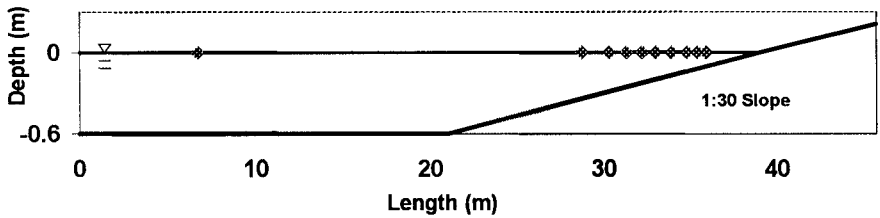

Figure 1. Flume layout. Symbols represent wave gauge locations.

Irregular waves were generated with a piston wave generator. Input wave spectra were generated with the parametric TMA spectral shape (Bouws et al. 1985) for single-peaked spectra and the linear combination of two TMA spectra for double-peaked spectra. Thirty-one wave conditions were run. The runs are summarized in Table 1. Peak wave periods (T_p) ranged from 1 to 2.5 sec and total energy-based wave heights (H_{mo}) were 0.09 or 0.06 m. For the double-peaked spectra, the higher frequency peak had a period of 1.0 sec and contained two-thirds of the total energy. The variation of the peak frequencies and heights provided a range of wave steepnesses. The widths of the frequency spectra were also varied. Spectral peakedness parameters (γ) of 3.3 (broad), 20, and 100 (narrow) were used. Data were sampled at 20 Hz for 600 sec. The first 50 sec of data was not analyzed to ensure the high-frequency components had reached Gauge 10. The data are band averaged to give 25 degrees of freedom.

Figure 2 shows measurements at Gauges 1, 6, and 10 for Runs 3, 11, 15, 26, and 28. These runs include double-peaked spectra (Runs 3, 11, and 15), narrow (Run 28) and broad (Run 26) single-peaked spectra, and total wave heights of 6 cm (Run 11) and 9 cm (Runs 3, 15, 26, and 28). All of these runs have a spectral peak at 0.57 Hz (1.75-sec period) and the double-peaked runs also have a peak at 1.0 Hz (1.0-sec period). At Gauge 1 in a depth of 61 cm, the spectra have substantial differences. Energies vary by one to two orders of magnitude in the region of the spectral peaks. At Gauge 10 in a depth of 5 cm, the waves are broken and the spectral shapes of all the runs are very similar, with the exception of the low frequencies (defined as the frequencies less than 0.3 Hz or half the incident peak period for these analyses). The surf zone results are consistent with the observations of Smith and Vincent (1992, 2003) who found that spectra in the inner surf zone reduce to a consistent equilibrium shape. At Gauge 6 in 15 cm water depth, only limited breaking occurs, but the wave spectra are evolving to very consistent shapes. Energy levels in the high-frequency tail are similar with only the lower energy run (Run 11) showing significantly lower magnitudes. Harmonics are also visible at a frequency near

1.14 Hz in all runs, but are most prominent in the narrower incident spectra (Runs 3, 11, and 28). Energy levels at the first harmonic are comparable for all cases at Gauge 6, whereas in that region the various runs differed by two orders of magnitude in the incident spectra. In Runs 3 and 11, the peak at 1 Hz was dominant in the incident spectra, but at Gauge 6, the 1-Hz peak is reduced and the 0.57-Hz peak is dominant.

Table 1. Laboratory wave conditions simulated.

Runs	Peak 1 T_p (sec)	Peak 2 T_p (sec)	H_{mo} (cm)	γ
1	2.5	1.0	9	20
2	2.0	1.0	9	20
3	1.75	1.0	9	20
4	1.5	1.0	9	20
5	1.25	1.0	9	20
6	2.0	-	9	20
7	1.5	-	9	20
8	1.0	-	9	20
9	1.25	1.0	6	20
10	1.5	1.0	6	20
11	1.75	1.0	6	20
12	2.0	1.0	6	20
13	2.5	1.0	6	20
14	1.25	1.0	9	3.3
15	1.75	1.0	9	3.3
16	2.5	1.0	9	3.3
17	1.25	1.0	9	100
18	1.75	1.0	9	100
19	2.5	1.0	9	100
20	1.0	-	9	3.3
21	1.0	-	9	20
22	1.0	-	9	100
23	1.25	-	9	3.3
24	1.25	-	9	20
25	1.25	-	9	100
26	1.75	-	9	3.3
27	1.75	-	9	20
28	1.75	-	9	100
29	2.5	-	9	3.3
30	2.5	-	9	20
31	2.5	-	9	100

Smith and Vincent (2003) examined only waves in the inner surf zone where significant dissipation occurred as well as strong nonlinear interactions. In laboratory experiments on relatively steep slopes, as presented here, it is difficult to separate the impacts of dissipation and nonlinear interactions on spectral shape. Thus, numerical experiments were conducted to fill this gap.

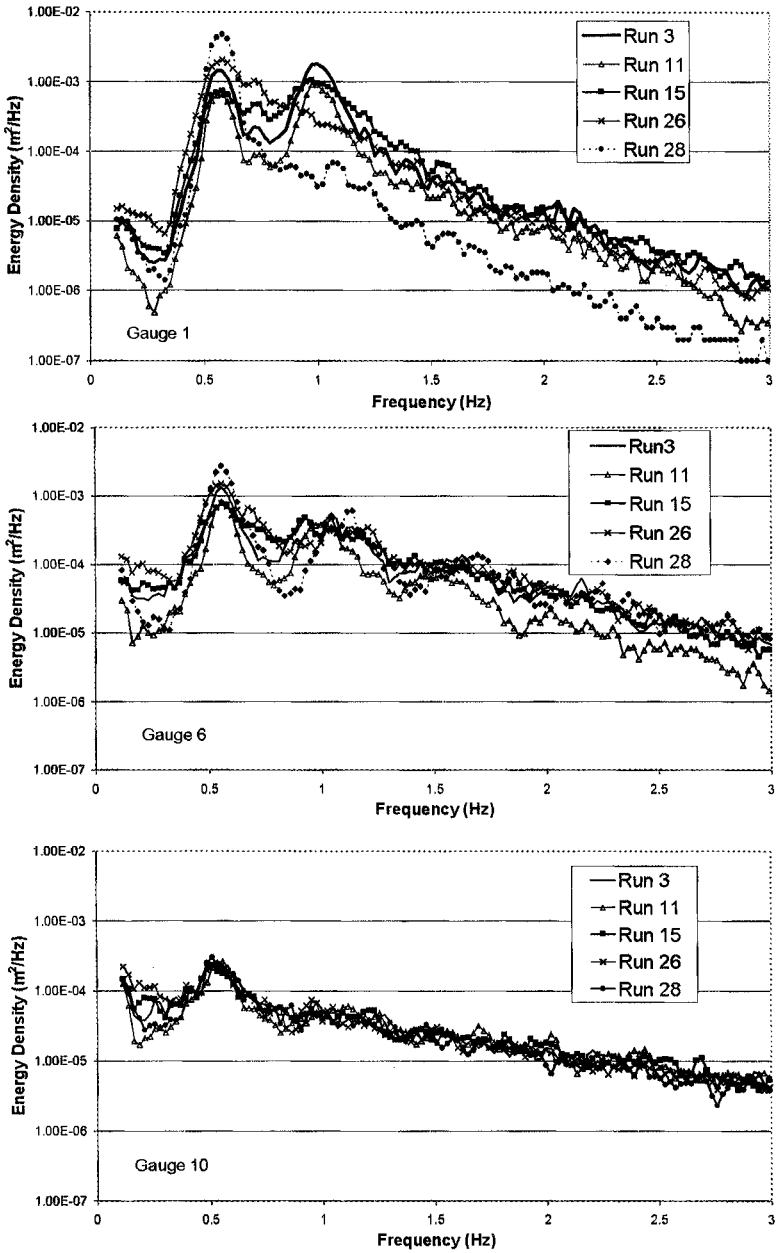

Figure 2. Measured spectral evolution at Gauges 1 (61-cm depth), 6 (15-cm depth), and 10 (5-cm depth) for Runs 3, 11, 15, 26, and 28.

3. Boussinesq Model Simulations

A one-dimensional Boussinesq model was used to simulate the laboratory flume experiments and then to investigate spectral evolution on a flat bottom. BOUSS-1D is based on the Boussinesq-type equations derived by Nwogu (1993) using the fully nonlinear form of Wei et al. (1995). The model is documented by Nwogu and Demirbilek (2001). BOUSS-1D is a time-domain model and includes surf zone wave breaking. A one-equation model is used to describe the turbulent kinetic energy produced by wave breaking and the effect of the dissipation is simulated through an eddy viscosity term, where the eddy viscosity is a function of the turbulent kinetic energy. Wave breaking is initiated when the horizontal component of the surface velocity exceeds the phase velocity. The numerical scheme is an implicit Crank-Nicolson scheme with a predictor-corrector method to give the initial estimate.

The results of BOUSS-1D were first compared to the laboratory experiments as validation to determine if the model could reproduce the spectral evolution observed in the lab. Next, the simulated spectra were examined to see if they reproduced the spectra equilibrium ranges observed by Smith and Vincent (2003). Finally, the model was run for the flat bottom case to isolate the spectral evolution due to nonlinear interactions. The model was run with default parameters and was not tuned to the laboratory data. The bottom friction was set to a very small value (Chezy coefficient, $C_f = 1000$) and the length scale for the eddy viscosity term was set to $l_t = 0.1$ m, which is approximately equal to the incident wave height. The spatial resolution was 0.05 m and the time step was 0.01 sec for all simulations.

Figures 3 and 4 show comparisons of the model to measurements for Runs 28 and 3, respectively. The spectra are shown for Gauges 1, 6, 8, and 10 at depths of 15, 9, and 5 cm, respectively. Run 28 has a single-peaked incident spectrum with a very narrow energy spread in frequency. At Gauge 6, just outside the breaking zone, strong harmonics are present in the spectra. In the mid surf zone (Gauge 8), the high frequency has filled out fairly uniformly and the harmonics are much less prominent. In the inner surf zone (Gauge 10), the high-frequency range is featureless (no apparent harmonic peaks). The model represents this evolution well in both spectral shape and energy density. Run 3 has a double-peaked incident spectrum with a moderate spread of energy in frequency. At Gauge 6, significant energy has been lost at the higher frequency peak. The energy density is 30 percent of that at the higher frequency peak in the incident spectra. At Gauge 10, the high-frequency range of the spectrum is featureless (as in Run 28) and the higher frequency peak is no longer

distinguishable. The model again represents this evolution in shape quite well, although the model over estimates the dissipation between Gauges 6 and 8.

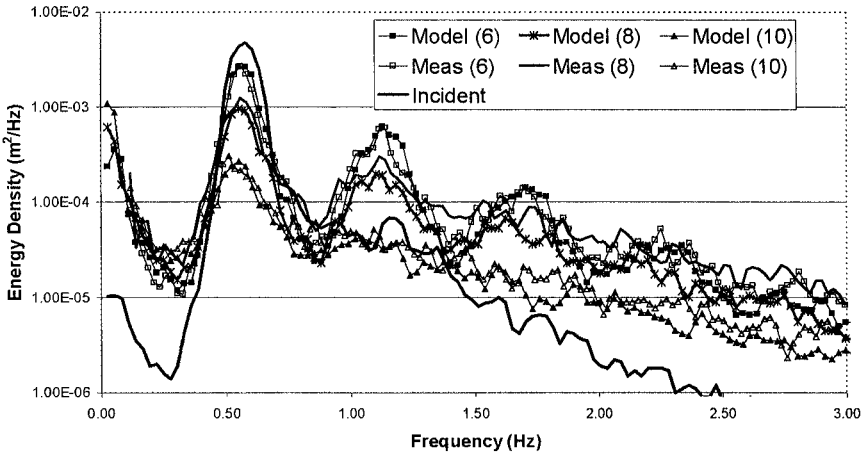

Figure 3. Measured and modeled spectra at Gauges 6 (15-cm depth), 8 (9-cm depth), and 10 (5-cm depth) for Run 28 (single peak).

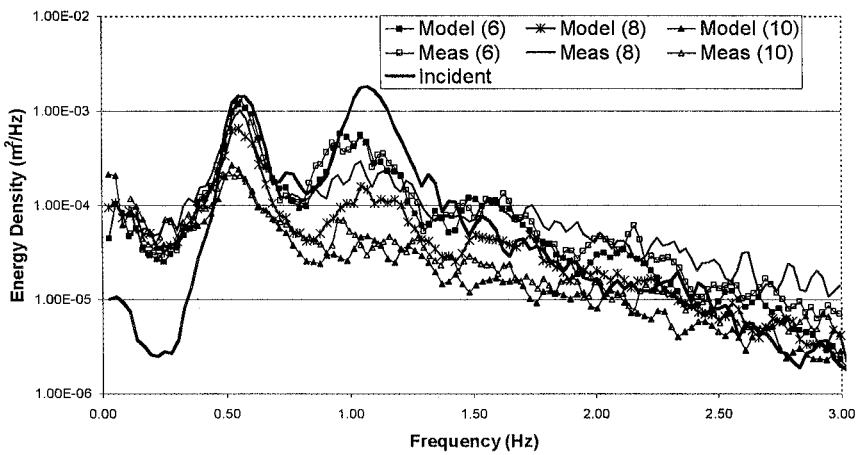

Figure 4. Measured and modeled spectra at Gauges 6 (15-cm depth), 8 (9-cm depth), and 10 (5-cm depth) for Run 3 (double peak).

The model replicates the laboratory measurements at Gauge 10 for the transformed spectra, and it also replicates the equilibrium range shapes observed by Smith and Vincent (2003) in the laboratory and field. Figure 5 shows the measured and modeled spectra in wave number space for Run 28,

Gauge 10. Frequencies were converted to wave numbers using linear wave theory. The equilibrium range slopes are superimposed on the plot. The plot is cut off at a *kd* value of 2, but the model tends to diverge to a slightly steeper slope at somewhat smaller wave numbers. Gauge 6 is also shown in the figure to illustrate the magnitude of the shape change.

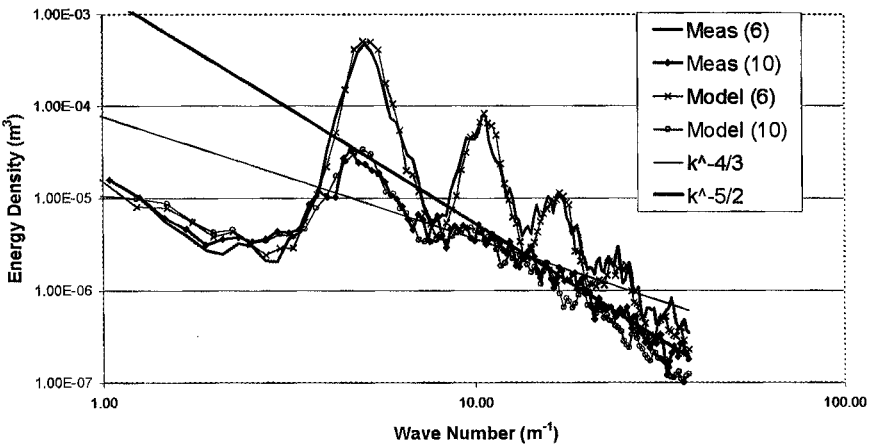

Figure 5. Measured and modeled spectral at Gauges 6 (15-cm depth) and 10 (5-cm depth) for Run 28 with equilibrium range slopes superimposed.

On the 1:30 plane slope, both the dissipation and nonlinear interaction source terms are strongly active, and from the measurements it is unclear which term is driving the evolution of the spectral shape. Numerical experiments on a flat bottom by Elgar et al. (1990) showed evolution to a featureless spectrum over distances of approximately 30 wavelengths. Norheim et al. (1998) showed that the equilibrium spectral shape evolved for large relative wave heights (e.g., H/d = 0.3), but not for smaller wave heights (e.g., H/d = 0.03). Additional numerical experiments were conducted using BOUSS-1D to investigate the evolution of the spectral equilibrium range over a flat bottom, where wave dissipation is secondary to wave-wave interactions. The bathymetry configuration for these simulations was similar to Figure 1, with a 20-m-long section of flat bed inserted in the slope at a water depth of 15 cm. The model was again driven with the water surface measurements at Gauge 1. An example of the spectral evolution along the flat-bottom section is shown in Figure 6 for the incident waves in Run 28. Spectra are shown for distances of one, three, five, and eight wavelengths (L) (based on the spectral peak) from the beginning of the flat section. The evolution to the featureless spectral shape

over a relatively short distance. By three wavelengths, the region $kd > 1$ has established an equilibrium shape, and by five wavelengths, the region $kd > 0.6$ has established an equilibrium shape. By eight wavelengths, the entire region above the peak has an equilibrium shape, and the peak has shifted down slightly. The model results are in agreement with the equilibrium shapes reported by Smith and Vincent (2003) ($k^{-4/3}$ for $kd < 1$ and $k^{-5/2}$ for $kd > 1$). For large wave numbers, $\sim k > 10$ or $kd > 1.5$, the slope produced in the model is $\sim k^{-7/2}$, steeper than the equilibrium slopes. At these relative depths, the model may start to under estimate the nonlinear interactions and is no longer appropriate. This is similar to the range where the model and laboratory data deviated.

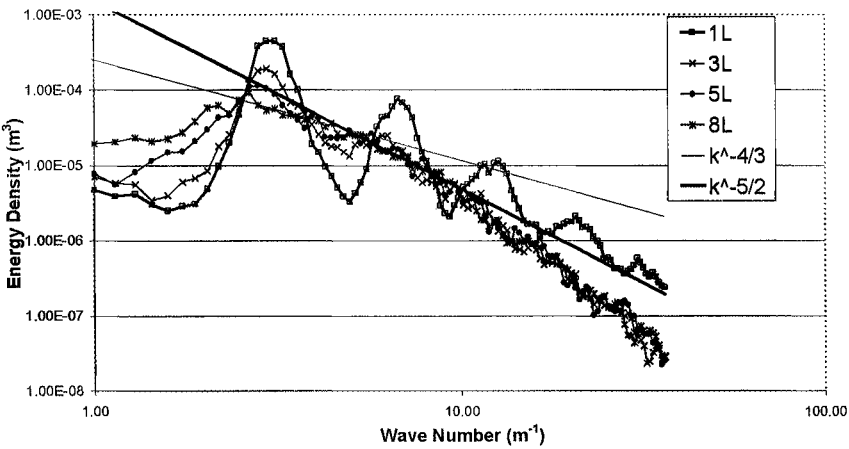

Figure 6. Modeled spectral evolution over a flat bottom at one, three, five, and eight wavelengths from the slope break with equilibrium slopes of Smith and Vincent (2003).

4. Discussion

The spectral equilibrium ranges observed by Smith and Vincent (2003) in the lab and field are replicated in the Boussinesq model on both a plane slope and a flat bottom. Spectra with multiple incident peaks and/or multiple strong harmonic peaks evolve over short distances to a featureless shape with slopes of $k^{-4/3}$ ($kd < 1$) and $k^{-5/2}$ ($kd > 1$). The evolution distance for the laboratory data simulated were typically three to five peak wavelengths. The evolution distance was a function of the spectral width and the relative wave height. Wider incident spectra and larger relative wave heights evolved to equilibrium over shorter distances. Spectra with multiple incident peaks evolved similar to the broader spectra. The equilibrium shapes evolved in cases with little or no wave

breaking, as well as with strong breaking. The evolution appears to be a function of nonlinear interaction, as speculated by Smith and Vincent. Broader spectral shapes drive interactions over a wider range of frequencies and speed up the evolution to equilibrium.

These simulations focused on the energy transfers to high frequencies, but substantial transfers also occur to low frequencies. The transfers feed not only the subharmonic of the spectral peak, but also tend to fill in all the frequencies below the peak. The trend again is toward a featureless spectrum. Figure 7 shows the simulated time histories of the water surface elevation for flat bottom simulations at two locations: 1) the slope break at 15 cm depth and 2) eight wavelengths along the flat bottom. The wave profile has changed from a strong vertical asymmetry with sharp crests and flat troughs to a strong horizontal asymmetry with forward leaning, saw-tooth waveforms. This is consistent with the evolution from a peaked spectrum with strong harmonics to a featureless spectrum with a broad equilibrium shape. The low-frequency nature of the wave train at the two locations is also different. At the slope break ($0L$ in Figure 7), the wave profile has a group structure, in which groups of high waves are followed by low waves, which are typical of narrow-banded spectra. At eight wavelengths ($8L$ in Figure 7), the individual waves are more consistent in amplitude, exhibiting a strong low-frequency oscillation.

5. Conclusions

Wave spectra of nonlinear, shallow-water waves outside the surf zone evolve to the same equilibrium shape observed in the surf zone. The equilibrium shape consists of two slopes, $k^{-4/3}$ for $kd < 1$ and $k^{-5/2}$ for $kd > 1$, as reported by Smith and Vincent (2003) in the surf zone. Broad incident spectra or multi-peaked spectra evolve to equilibrium over shorter distances than narrow incident spectra. Likewise, the evolution distances shorten as nonlinearity increases. For the incident conditions given in Table 1, evolution distances were $3L$ to $5L$ (wave heights of 6-9 cm) in a depth of 15 cm. The one-dimensional, time-domain Boussinesq model of Nwogu and Demirbilek (2001) reproduced the spectral evolution both inside and outside the surf zone. The model also reproduced the equilibrium range spectral shapes for $kd < 1.5$. Similar to deepwater spectral evolution, the equilibrium range in shallow water is driven by the nonlinear wave-wave interactions. The evolution in spectral shape from strong harmonic peaks to an equilibrium shape reflects the change in wave shape from a vertical asymmetry to a horizontal asymmetry. The low frequency energy also grows through the evolution, both inside and outside the surf zone.

Acknowledgments

Permission to publish this paper was granted by the Office, Chief of Engineers, U.S. Army Corps of Engineers. This research was conducted under the Transformation-Scales Waves work unit in the Navigation Systems Program of the Coastal and Hydraulics Laboratory (CHL), U.S. Army Engineer Research and Development Center (ERDC). Jeffrey Melby, CHL-ERDC, conducted laboratory experiments. Okey Nwogu, University of Michigan, and Zeki Demirbilek, CHL-ERDC, assisted with numerical simulations.

References

Booij, N., R. C. Ris, and L. H. Holthuijsen. 1999. A third-generation wave model for coastal regions, Part I, Model description and validation. *J. Geophys. Res.*, Vol 104, No. C4, 7649-7666.

Bouws, E. H. Gunther, W. Rosenthal, and C. L. Vincent. 1985. Similarity of the wind wave spectrum in finite depth waver; 1. Spectral form, J. Fluid Mechanics, 158, Sep., 47-70.

Eldeberky, Y. and J. A. Battjes. 1996. Spectral modeling of wave breaking: application to Boussinesq equations, *J. Geophys. Res.*, 101(C1), 1253-1264.

Elgar, S., M. H. Freilich, and R. T. Guza. 1990. Recurrence in truncated Boussinesq models for nonlinear waves in shallow water, *J. Geophys. Res.*, 95(C7), 11547-11556.

Herbers, T. H. C. and M. C. Burton. 1997. Nonlinear shoaling of directionally spread waves on a beach, *J. Geophys. Res.*, 102(C9), 21101-21114.

Norheim, C. A., T. H. C. Herbers, and S. Elgar. 1998. Nonlinear evolution of surface wave spectra on a beach, *J. Phys. Ocean.*, 28, 1534-1551.

Nwogu, O. G. 1993. Alternative form of Boussinesq equations for nearshore wave propagation. *J. Wtrways., Port, Coast. and Oc. Engrg.*, 119(6), 618-638.

Nwogu, O. G., and Z. Demirbilek. 2001. Boussinesq wave model for coastal regions and harbors. Technical Report ERDC/CHL TR-01-25, US Army Engineer Research and Development Center, Vicksburg, MS.

Resio, D. T., J. H. Pihl, B. A. Tracy, and C. L. Vincent. 2001. Nonlinear energy fluxes and the finite depth equilibrium range in wave spectra. *J. Geophys. Res.*, Vol. 106, No. C4, 6985-7000.

Smith, J. M., and C. L. Vincent. 1992. Shoaling and decay of two wave trains on a beach. *J. Wtrways., Port, Coast. and Oc. Engrg.*, 118(5), 517-533.

Smith, J. M., and C. L. Vincent. 2002. Application of spectral equilibrium ranges in the surf zone. *Proc., 28th International Conference on Coastal Engineering*, World Scientific, 269-279.

Toba, Y. 1973. Local balance in the air-sea boundary processes on the spectrum of wind waves, *J. Oceanogr. Soc. Jpn.*, 29, 209-220.

Wei, G., J. T. Kirby, S. T. Grilli, and R. Subramanya. 1995. A fully nonlinear Boussinesq model for surface waves, Part 1, highly nonlinear unsteady waves. *J. Fluid Mech.*, 294, 71-92.

Zakharov, V. 1999. Statistical theory of gravity and capillary waves on the surface of a finite-depth fluid. *Eur. J. Mech. B/Fluids*, Vol. 18, Issue 3, 327-344.